# SEPARATED FLOW

W. L. Sellers, III,
R. E. Dunham, Jr.,
W. L. Goodman,
F. G. Howard,
R. J. Margason,
D. H. Rudy,
C. L. Rumsey,
H. P. Stough, III, and
J. L. Thomas
NASA Langley Research Center
Hampton, Virginia

Abstract

This paper provides a brief overview of flow separation phenomena. Langley has many active research programs in flow separation related areas. Most of these programs were reviewed for inclusion in this paper. Three cases were selected which describe specific examples of flow separation research. In each example, a description of the fundamental fluid physics and the complexity of the flow field is presented along with a method of either reducing or controlling the extent of separation. The following examples are discussed in the present paper: (1) flow over a smooth surface with an adverse pressure gradient; (2) flow over a surface with a geometric discontinuity; and (3) flow with shock-boundary layer interactions. These results will show that improvements are being made in our understanding of flow separation and its control.

## Flow Separation

Flow separation is an important fluid dynamic problem which can cause a drastic reduction in the performance of aircraft, diffusers, pumps and compressors. The resulting flow fields are also some of the most complex to measure since they typically include regions with steep velocity gradients and unsteadiness as well as bidirectional or reverse flow.

This paper provides a brief overview of flow separation phenomena. Langley has many active research programs in flow separation related areas. Most of these programs were reviewed for inclusion in this paper. Three cases were selected which describe specific examples of flow separation research. In each example, a brief description of the fundamental fluid physics and the complexity of the flow field is presented along with a method for either reducing or controlling the extent of separation. The following examples are discussed in the present paper: (1) flow over a smooth surface with an adverse pressure gradient; (2) flow over a surface with a geometric discontinuity; and (3) flow with shock-boundary layer interactions.

The classical description of flow separation usually states that, in general, for separation to occur the fluid must be subjected to an adverse pressure gradient (increasing pressure) with laminar or turbulent viscosity effects. The energy in the low momentum fluid in the boundary layer is expended in overcoming the rise in pressure. Eventually the surface streamline reaches a point where the shear stress at the wall reaches zero ($\frac{\partial u}{\partial y} = 0$) and the streamline breaks away from the surface. This description represents a considerable over-simplification of the process and may only be applicable to perhaps the simplest of two-dimensional steady separation cases. The modern concept of separation describes the process as beginning intermittently at a given location with the actual streamline detachment point occurring over a zone.

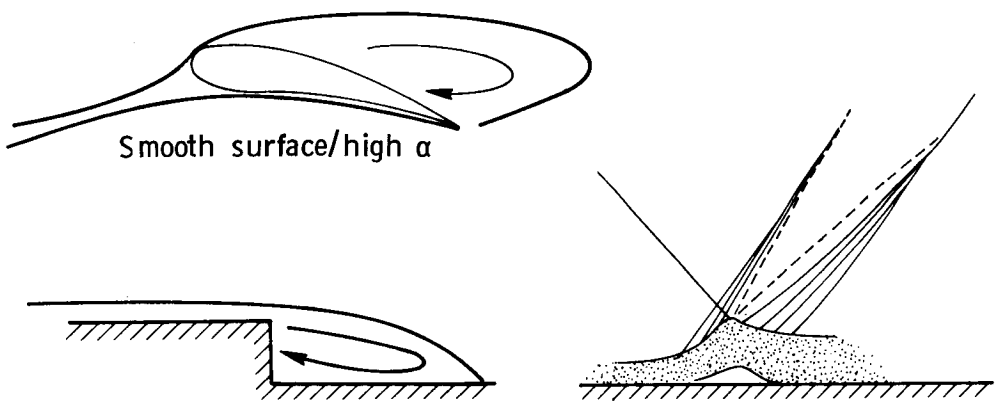

## 2D Airfoil Separation Analysis

An airfoil at a high angle of attack provides an example of separation from a smooth surface with an adverse pressure gradient. In this case, separation is usually a gradual process with the stall region increasing up to the point of $C_{Lmax}$. Separation is further complicated by the formation of laminar leading-edge bubbles which may be of either the short or long bubble type. The long bubble may trigger the transition of the boundary layer to a turbulent layer near the reattachment point, whereas the short bubble separation may contract and burst leading to massive upper surface separation.

Additional complications may occur at angles of attack beyond that required to obtain $C_{Lmax}$. The figure shows the separation characteristics of an NACA 0012 airfoil at 18 degrees angle of attack and a chord Reynolds number of 1 million. The experimental data are compared with solutions of the thin-layer Navier-Stokes equations which were obtained by Chris Rumsey.[1] The calculations show very good agreement with experimental data and also illustrate another phenomenon which is not well defined by experiment. The experimental data show a gradual increase in lift up to a maximum $C_L$ of 1.53 at an angle of attack of 16.9 degrees; then a drastic loss of lift as angle of attack is increased further. At angles of attack greater than that required to achieve $C_{Lmax}$, the calculations predict an unsteady solution. The separation bubble located above the airfoil leading edge alternately grows and shrinks with respect to time as illustrated in the figure. The vector plots correspond to the minimum and maximum lift coefficient values in the shedding cycle. When the calculations are time averaged, they show very good agreement with the mean values of the experimental data. Experiments designed to measure separated flows must strive to measure the unsteady features as well as the mean or time-averaged quantities.

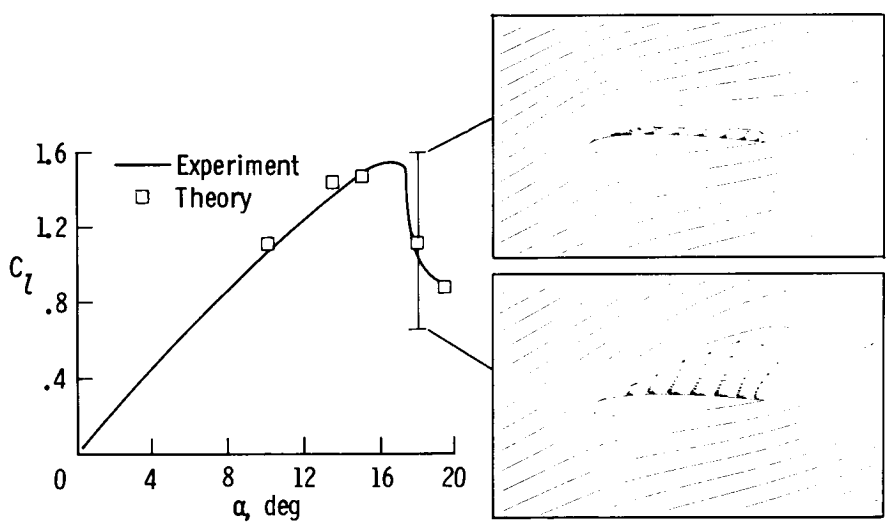

## 3D Wing Separation

The complexity of the flow field increases as three-dimensional effects are included. Recent experimental investigations have provided new insight into the complex nature of flow separation on wings and wing bodies.[2] The left half of the figure shows results obtained by Winkelmann[3] in which he photographed fluorescent oil flow on a series of simple, unswept, rectangular planform wings of whose aspect ratios ranged from 3 to 12. All of the wings had a 3.5 in chord and a 14 percent thick Clark-Y airfoil section. Test conditions correspond to a chord Reynolds number of 385,000 and an angle of attack of 18.4 degrees. The oil flow patterns on all three wings show a "bead-like" pattern near the wing leading edge which indicates the presence of a laminar leading-edge separation bubble. The aspect ratio 3 wing illustrates the presence of one large "mushroom" stall cell on the upper surface of the wing. A close examination of the oil pattern indicates that only at the centerline of the wing could the flow pattern even remotely be called two-dimensional. There are indications of strong spanwise flow everywhere else on the wing along with vortical flow nodes near both mid semispan positions. An increasing number of "mushroom" cells are observed as the wing aspect ratio is increased; in addition it is not apparent that the flow tends toward two-dimensional characteristics with increased aspect ratio. In this investigation relatively symmetrical patterns are observed on the wings.

The addition of a body to a configuration results in a more complicated flow field. In a recent investigation by Sellers and Kjelgaard, (NASA Langley Research Center, unpublished data) oil flow patterns were observed on an aspect ratio 7 wing with a 14 in chord NACA 0012 airfoil section. The wing was mounted in a high-wing position on a small cylindrical body as shown in the upper right portion of the figure on the next page. Test conditions corresponded to a chord Reynolds number of 1 million with angle of attack ranging from 6 to 22 degrees. The oil flow pattern on the upper surface of the wing at an angle of attack of 20 degrees is shown in the lower right of the figure. A complex and asymmetrical pattern develops with large regions of reverse flow on each wing and spiral nodes forming from the flow at the wing-body juncture. The oil flow patterns change dramatically as the angle of attack is increased above $C_{L_{max}}$. At 16 degrees angle of attack the flow pattern is steady and asymmetric with only the left wing separated. At 17 degrees angle of attack, an unsteady separation occurs where the left wing remains separated and the right wing alternates between attached and separated flow. Between 18 and 20 degrees the pattern remains steady and asymmetric as shown in the lower right of the figure. Two features from these photographs are noteworthy: (1) the flow separation patterns are very complex and three-dimensional; and (2) the small fuselage appears to cause large flow asymmetries which were not apparent in Winkelmann's observations on wings without bodies. These asymmetries are expected to be more significant with larger bodies and with more complex configurations.

3D Wing Separation



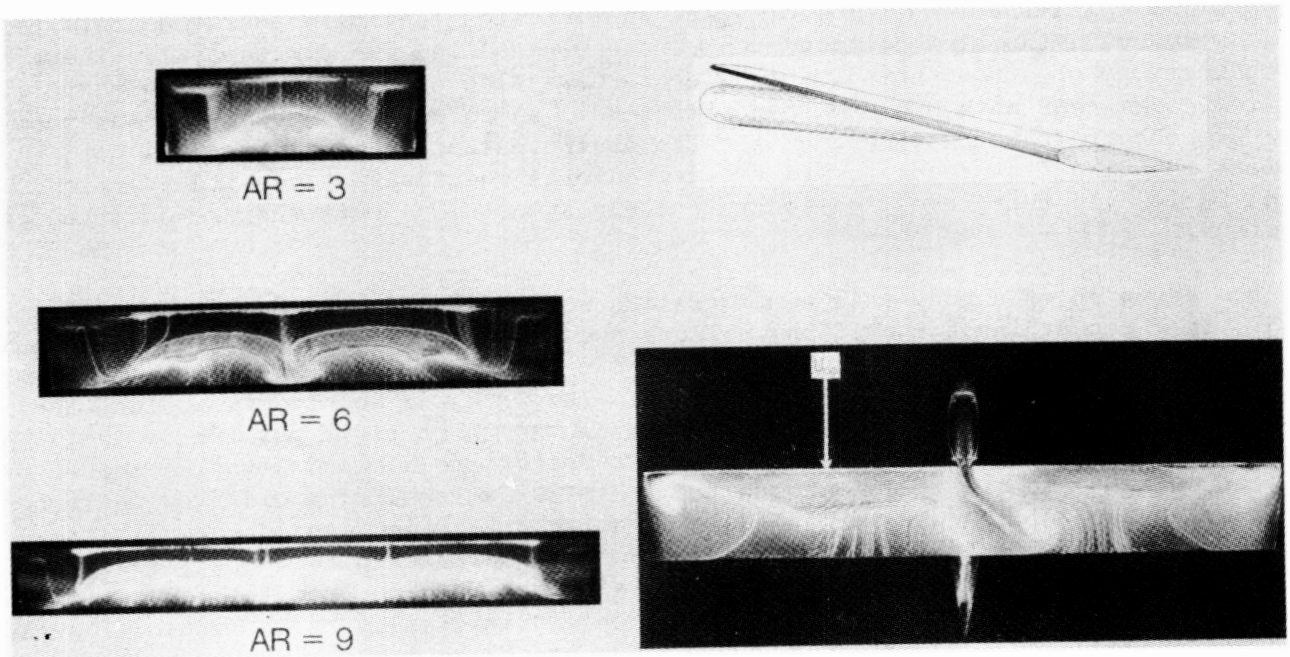

## Two-Phase Flow Induced Separation

NASA is conducting research to find if heavy rain concentration is a factor in airfoil flow separation.[4] Analysis has shown that significant increases in drag can occur when an aircraft encounters rain with liquid water content from 15 to 60 $g/m^3$, which corresponds to between 19 and to 70 in of rain per hour. Flight measurements have demonstrated that these levels can be encountered during thunderstorms.

A preliminary experiment was conducted in the Langley 4- by- 7 meter tunnel to investigate the sensitivity of airfoil performance to heavy rain encounters. The sketch on the left side of the of the figure illustrates the experimental setup. For this test, a 2.5 ft chord NACA 64-210 airfoil was installed in the aft portion of the test section and a water spray manifold system was located in the forward part of the test section. The spray system was capable of generating a two-phase flow of 4.5 percent water by weight, which is equivalent to 57 in of rain per hour.

The right side of the figure shows the section lift coefficient data obtained at a Reynolds number of 2.6 million. The baseline data (water spray off) indicated that stall was beginning to occur at an angle of attack of about 18 to 20 degrees. For the highest spray rate (4.5 percent water by weight or 57 in/hr) the data indicate that separation begins at a lower angle of attack and that stall occurs at an angle of attack of 12 degrees. The maximum lift coefficient is reduced by 25 percent.

Continuing tests will attempt to identify the mechanisms which cause premature separation in two-phase flow and to determine the sensitivity of full scale wings to these phenomena.

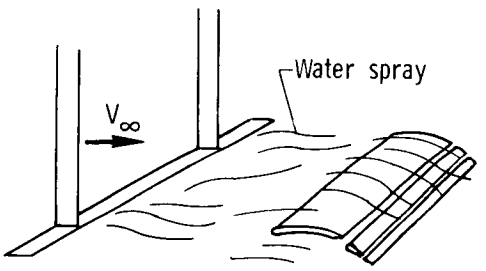


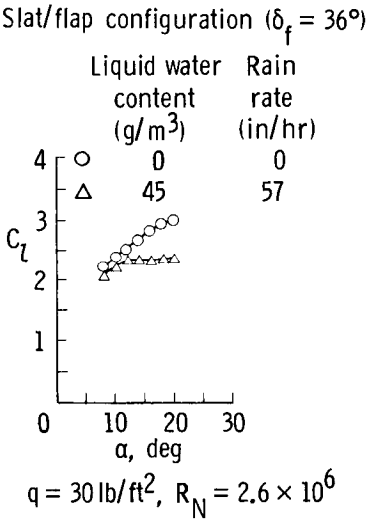

## Leading-Edge Droop Separation Control

NASA Langley is conducting research oriented toward improving the spin resistance of light airplanes.[5] The research has shown that the addition of a discontinuous, outboard wing leading-edge droop can provide significant improvements in aircraft stall characteristics and spin resistance. Wind tunnel tests at NASA Langley and the University of Maryland explored the effect of these wing leading-edge modifications and flight tests have verified the results.

The graph on the left side of the figure shows the variation of the total resultant force coefficient for the outer wing panel $C_{r_{o.w.}} = (C_L^2 + C_D^2)^{1/2}$ versus angle of attack from a 1/6 scale wind tunnel model at a Reynolds number of 320,000. Resultant force is more relevant to autorotative characteristics than lift, at high angles of attack. A negative resultant force curve slope is indicative of unstable roll damping and a tendency to spin. The addition of the leading-edge droop has a negligible effect on the resultant force coefficient at low angles of attack. Beyond the stall angle of the basic wing, however, the lift of the modified wing continues to increase and produces a stabilizing force slope up to 30-35 degrees angle of attack. The fluorescent oil flow visualization photographs on the right side of the figure show the effect of the leading-edge droop on the flow patterns on the wing. A close examination of the photographs shows a vortex-type flow emanating from the leading-edge discontinuity which prevents the outward progression of the separated flow.

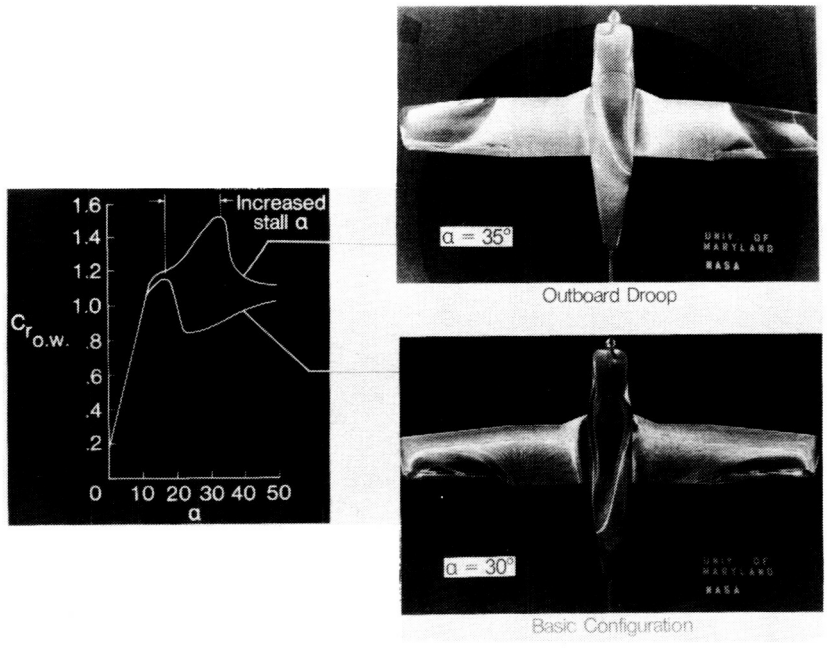

## Blunt Body Separation Analysis

The separated flow in the base region of a blunt body produces a drag force which can contribute significantly to the total drag of the body. In general, the nature of the near-wake flow is strongly dependent upon the geometry of the body and the Mach number regime and Reynolds number of the external flow. For example, a two dimensional bluff body in a subsonic stream generates a wake dominated by alternately shed vortices over a wide range of Reynolds numbers. Since the base drag in this case is associated with the vortex shedding, methods for reducing the base drag must be directed toward eliminating or weakening the vortex shedding or delaying the formation of the vortices. Two of the methods that have been found to reduce base drag in wind tunnel experiments are being studied numerically using solutions of the time-dependent Navier-Stokes equations. These two methods include the use of either a base cavity or the injection of mass through the base into the wake. The finite-difference scheme used in the present study is the unsplit MacCormack (ref. 6) explicit predictor-corrector technique which can be vectorized efficiently for calculations which use the CDC VPS-32 computer at Langley.

Shown in the figure are calculations of subsonic flow for a slender body with and without a rectangular base cavity.[7] Velocity vectors are shown in the near-wake region, for Mach 0.6 flow with a Reynolds number based on chord length of $9.62 \times 10^3$, at a point in time after periodic flow has been established. The presence of the cavity allows the vortex formation region to extend into the cavity. As a result, the pressure along the rear wall of the cavity is now higher than that along the base of the unmodified configuration which reduces the base drag.

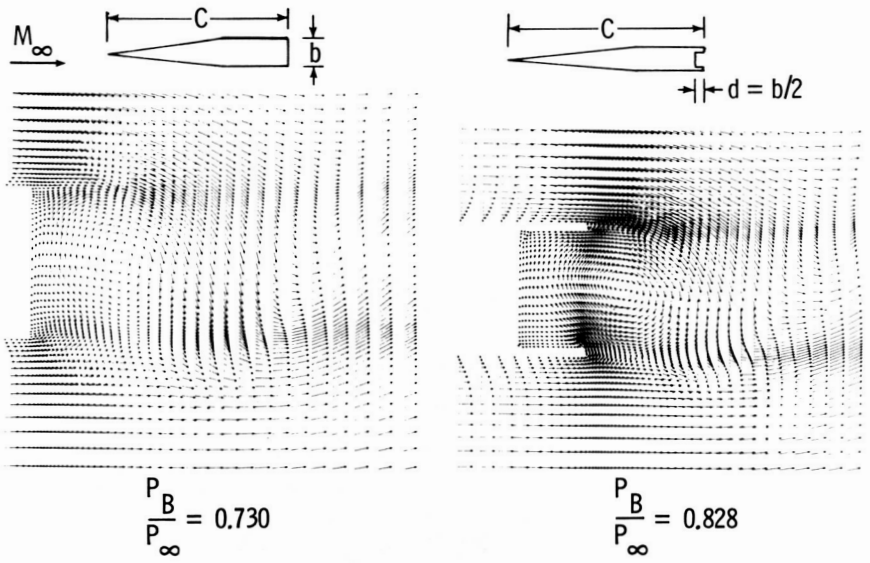

## Bluff Body Separation Control

The drag of afterbodies in fluid flow can be kept low if the closure angle is low enough that attached flow is maintained over the afterbody (streamline body).[8] However, in many situations this approach is not practical because the length required becomes excessive. Therefore, in these situations (such as ground transportation) the afterbodies are typically truncated rather sharply. The parameter which causes separation is the magnitude of the adverse pressure gradient which occurs in the region where the flow is being expanded. Non-attached (or separated) flow on an axisymmetric bluff afterbody is shown in the photo on the upper right (flow from left to right). It can be seen that separation occurs just downstream of the shoulder of the body boattail. This separated flow results in high drag as shown by the drag measurements for the non-grooved bluff afterbody. Previous investigations have indicated that transverse grooves can be effective in delaying separation for two-dimensional diffusers (internal flow). The photo on the lower right illustrates how the flow remains attached over a much greater region of the bluff afterbody when transverse grooves are employed in the shoulder region. Measurements show that the better flow attachment reduces drag coefficient measurements at intermediate Reynolds numbers (approximately 0.3 to 1.3 x 105) for the grooved afterbody. The mechanism of the transverse grooves appears to be one of substituting several small regions of separation (which provide a wall slip boundary condition) for a larger separated flow region. It appears that the grooves should be located in the region of high longitudinal pressure gradient. The grooves may need to be tailored to provide a reduced drag coefficient at a particular Reynolds number.

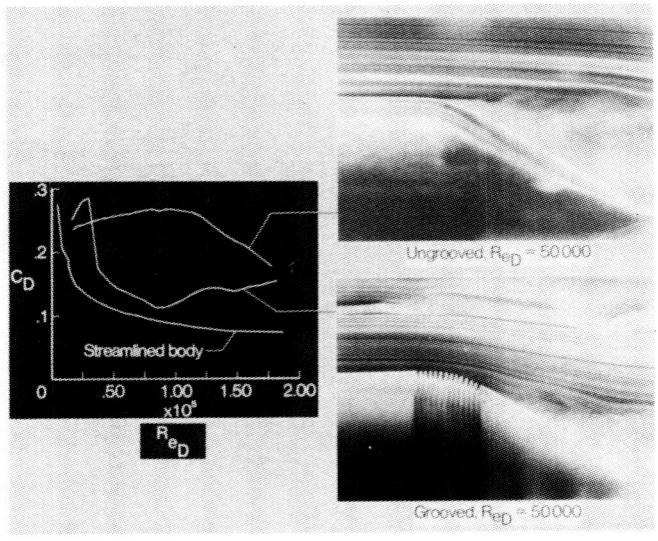

## Shock-Boundary Layer Interaction

As the velocity increases over a body, shock waves form and interact with the boundary layers developing near the surface. If the shock wave is weak, the flow remains attached and the effect of the thickening boundary layer is to convert the sharp pressure rise into a more gradual one. If the shock wave is of sufficient strength, the boundary layer will separate due to the strong adverse pressure gradient through the shock. The interaction region, in the case of laminar boundary layer separation, is larger than that for a turbulent boundary layer separation.[9]

The separation of a boundary layer due to an impinging shock wave is a classical example of the process and can commonly occur in supersonic inlets. The analysis of Thomas and Wallace[10] corresponds to the experiments of Hakkinen et al.[11] at a free-stream Mach number of 2.00 and a Reynolds number based on the length from the leading edge to the shock impingement point of 2.96 × 105. The pressure contours are prepented on the left of the figure and show several distinct features of this flow. The oblique shock formed at the leading edge of the plate is shown at x/L = 0. The impinging shock intersects the plate at x/L = 1.0 and is of sufficient strength to cause separation of the laminar boundary layer. The interaction region is large compared to the boundary layer thickness and encompasses the region from x/L = 0.77 to 1.15. In the separated zone, the plateau region of nearly constant static pressure is evident. The streamlines and velocity vectors in the vicinity of the interaction region are shown on the right of the figure. A separation bubble with reversed flow is shown in the interaction region.

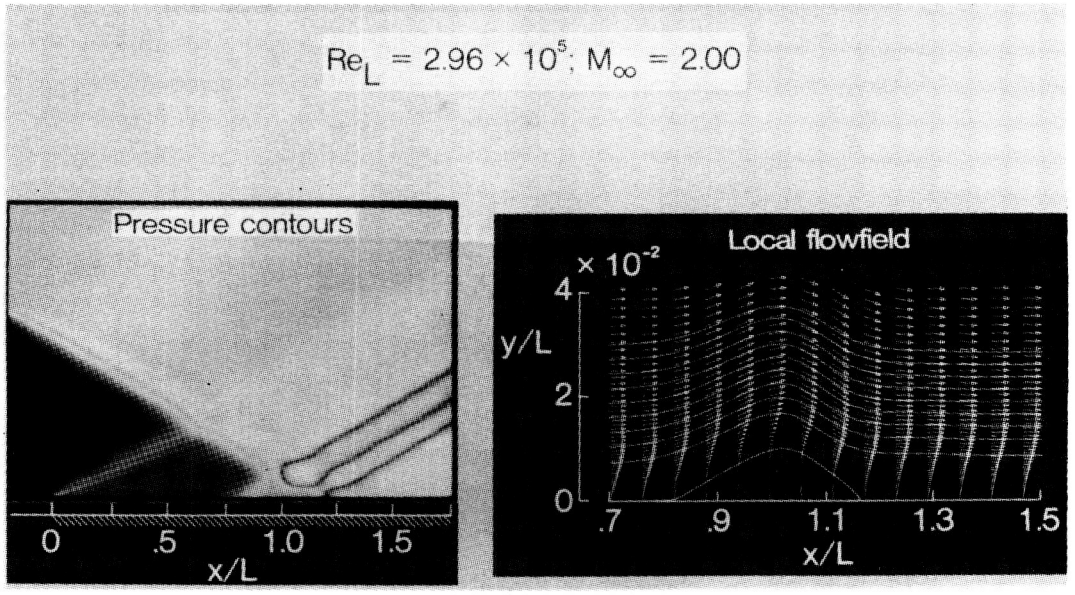

## Control Plate for Shock-Boundary Layer Interaction

Numerical and experimental studies have been done on a new, passive approach for separation control in shock-boundary layer interaction.[12] The device consists essentially of a horizontal plate suspended in the outer part of the boundary layer. This plate is positioned such that the incident shock reflects from this plate rather than the wall, thus effectively shielding the low momentum flow near the wall from the tremendous adverse pressure gradient engendered by shock impingement.

The figure shows a plot of the normalized wall static pressure versus the distance downstream on the experimental test plate along with the corresponding Schlieren photograph of the flow field with the control plate in place. The square symbols correspond to the reference case without the control plate and the diamond symbols correspond to the case with the control plate. From this plot it can be seen that with the addition of the control plate the interaction region has been shortened. Further investigations will be conducted to identify the total drag reduction.

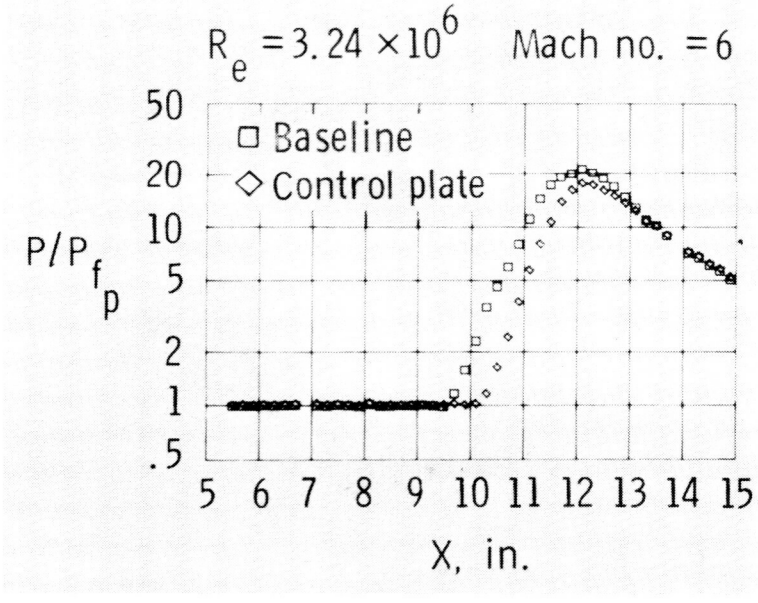


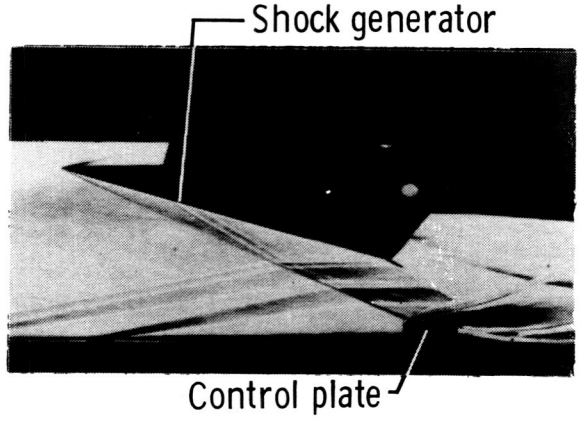

Summary

Flow separation generated by an airfoil or an aircraft at high angles of attack is an extremely complicated process. The basic physics are becoming better understood, but additional research is required. NASA Langley has recently started an experimental and analytical effort directed toward understanding the complexities of flow separation. Related research is also providing information on how to control separation with simple yet effective modifications to wing leading edges and on the effect of very heavy rain on flow separation.

Flow separation from blunt bases or bluff bodies represents a significant portion of body drag. For the case of the blunt base, vortex shedding is the dominant feature which produces higher base pressures and thereby larger drag. Recessing the base to form a cavity has been shown both experimentally and numerically to reduce the base drag. Spanwise grooves have been shown to reduce flow separation on bluff bodies.

Shock-boundary layer interactions commonly occur at high speed and can seriously degrade the performance of engine inlets and diffusers. A small control plate to shield the boundary layer from the impinging shock has been effective in modifying the interaction region.

OVERALL OBJECTIVES - BETTER UNDERSTAND THE FUNDAMENTAL PHYSICS AND TO IDENTIFY EFFECTIVE SEPARATION CONTROLS

- HIGH-$\alpha$
  - HEAVY RAIN AGGRAVATES FLOW SEPARATION
  - LEADING EDGE DROOP REDUCES SEPARATION IN OUTBOARD REGIONS
- BLUNT/BLUFF BODY SEPARATION
  - BASE CAVITY REDUCES BASE DRAG
  - SPANWISE GROOVES REDUCE SEPARATION ON BLUFF BODIES
- SHOCK-BOUNDARY LAYER INTERACTION
  - CONTROL PLATE CAN DELAY SEPARATION

## References


1. Christopher L. Rumsey: Time-Dependent Navier-Stokes Computations of Separated Flows Over Airfoils. AIAA Paper No. 85-1684, July 1985.

2. Richard J. Margason: Computational Methods for Subsonic Aerodynamic Flow Separation. 4th International Conference on Applied Numerical Modeling, Tainan, Taiwan, December 1984.

3. A. E. Winkelmann: On the Occurrence of Mushroom Shaped Stall Cells in Separated Flow. AIAA Paper No. 83-1734, July 1983.

4. R. Earl Dunham, Jr., Gaudy M. Bezos, Garl L. Gentry, Jr., and Edward Melson, Jr.: Two-Dimensional Wind Tunnel Tests of a Transport-Type Airfoil in a Water Spray. AIAA Paper No. 85-0258, January 1985.

5. H. Paul Stough, III, Daniel J. DiCarlo, Kenneth E. Glover, and Eric C. Stewart: Wing Design for Spin Resistance. AIAA Paper No. 84-2223, July 1984.

6. MacCormack, R. W.: The Effect of Viscosity in Hypervelocity Impact Cratering. AIAA Paper 69-354, April 1969.

7. David H. Rudy: Navier-Stokes Solutions for Two-Dimensional Subsonic Base Flow. Southeastern Conference on Theoretical and Applied Mechanics, Pine Mountain, Ga., May 1984.

8. F. G. Howard, W. L. Goodman, and M. J. Walsh: Axisymmetric Bluff-Body Drag Reduction Using Circumferential Grooves. AIAA Paper No. 83-1788, July 1983

9. P. K. Chang: Control of Flow Separation: Energy Conservation, Operational Efficiency, and Safety. McGraw-Hill Book Co., Washington, D.C., 1976.

10. James L. Thomas and Robert W. Walters: Upwind Relaxation Algorithms for the Navier-Stokes Equations. AIAA Paper No. 85-1501, July 1985.

11. R. J. Hakkinen, I. Greber, L. Trilling, and S. S. Abarbanel: The Interaction of an Oblique Shock Wave with a Laminar Boundary Layer. NASA Memo-2-18-59W, March 1959.

12. W. L. Goodman, E. L. Morrisette, M. Y. Hussaini and D. M. Bushnell: Control Plate for Shock-Boundary Layer Interactions. AIAA Paper No. 850523, March 1985.


C-5